Haggerty, J.A., Premoli Silva, I., Rack, F., and McNutt, M.K. (Eds.), 1995
*Proceedings of the Ocean Drilling Program, Scientific Results,* Vol. 144

# 21. STRONTIUM ISOTOPE VARIATIONS AND SEDIMENT REWORKING OF THE UPPER OLIGOCENE–NEOGENE INTERVAL FROM SITES 871 AND 872[1]

Carsten Israelson,[2] Paul N. Pearson,[3] and Bjørn Buchardt[2]

## ABSTRACT

Strontium isotopes were used to evaluate the subsidence and sedimentation history of Limalok and Lo-En guyots in the western Pacific Ocean. We found that the Sr-isotope data from pelagic sediments deposited after the drowning of the guyots not only reflect the variations in seawater isotopic composition during the Neogene but also the amount of sediment reworking. At Site 871 (Limalok Guyot ), analyses from the complete pelagic cap were obtained; however, at Site 872 (Lo-En Guyot), only the lowermost 50 m of the pelagic cap was analyzed. Limalok Guyot subsided and started to accumulate pelagic sediments about 20 Ma; Lo-En Guyot started at about 27 Ma. Sediment accumulation was not continuous, and sediments were considerably reworked at several intervals. In general, sediment reworking occurs during the initial pelagic sedimentation. On Limalok Guyot, another interval of sediment reworking as well as large erosional intervals from 14.2 to 2.4 Ma were identified.

## INTRODUCTION

### Strontium Isotope Stratigraphy

The Cenozoic Sr-isotope variations in seawater were first described by Burke et al. (1982), and additional data were given by Koepnick et al. (1985, 1988). The Neogene part of the Sr-isotope seawater curve has recently received attention (DePaolo, 1986; Hess et al., 1989; Hodell et al., 1989, 1990, 1991; Miller et al., 1988, 1991; Hodell and Woodruff, 1994; Oslick et al., 1994). These advances have allowed the development of a detailed marine Sr-isotope chronology for the Neogene and the Oligocene based on high precision measurements of well-dated Deep Sea Drilling Project (DSDP) and Ocean Drilling Program (ODP) sites. The most promising interval for high temporal resolution during the Cenozoic is the early Miocene, for which the Sr-isotope seawater curve exhibits the greatest rate of change in $^{87}Sr/^{86}Sr$ with time (Hodell and Woodruff, 1994).

The original purpose of this study was to apply the existing, well-dated, Sr-isotope seawater curve to the pelagic sediments from Sites 871 and 872 and thus establish an Sr-isotope chronology for these sites. Because Sites 871 and 872 contain an extended lower Miocene interval with an insufficient biostratigraphic resolution, Sr isotopes were considered a useful dating tool. However, because several intervals of the pelagic caps at these sites have been severely reworked (Pearson, this volume; Pearson and Shackleton, this volume), an interpretation of the Sr-isotope values is hampered. Instead, part of the data have been applied as an indicator of reworking of the pelagic sediments.

### Location and Drilling Summary

The two sites investigated are located at Limalok and Lo-En guyots (see site map preceding title page). Limalok (Harriet) Guyot is situated in the southern part of the Marshall Islands at 5°33.4′N, 172°20.7′E and is considered the youngest of the guyots in the Marshall Islands. Lo-En Guyot is located at 10°5.6′N, 162°52.0′E, in the northern part of the Marshall Islands, approximately 148 km south from Anewetak Atoll. Lo-En Guyot and the living Anewetak Atoll are bathymetric features sharing the same volcanic pedestal.

Pelagic caps accumulated on the guyots after they subsided below sea level. The pelagic sediments have remained well above the carbonate compensation depth and contain a well-preserved Oligocene to Neogene foraminifer fauna. At Limalok (Site 871), samples from the entire pelagic cap were analyzed, whereas only samples from the lowermost 50 m of the pelagic cap at Lo-En (Site 871) were studied. The samples from Lo-En Guyot included the Miocene/Oligocene boundary, which is not represented at Limalok Guyot.

Site 871 was drilled through the central and thickest part of the pelagic cap of Limalok Guyot at a water depth of 1255 m. The pelagic sediments were cored using the advanced hydraulic piston corer (APC) in two holes (871A and 871B). The most complete recovery of pelagic sediments (90.7%) was obtained in Hole 871A, which also provided all of the samples from Site 871 that were analyzed for this study. At Hole 871A, refusal occurred at 139.5 meters below seafloor (mbsf) as the piston core reached the Eocene limestone platform below. The platform limestone was thereafter drilled using the extended core barrel (XCB) to a total depth of 151.9 mbsf, with a recovery of only 2.4%. The top of the carbonate platform and the contact with the pelagic sediments above is marked by a black, laminated, iron-manganese crust.

Site 872 was drilled at the central and thickest portion of Lo-En Guyot at a water depth of 1084 m. Two adjacent holes (872A and 872C) were cored through the pelagic cap using the APC. Hole 872C was the most complete hole drilled at this site, with a pelagic sediment recovery of 97.7%; the samples used in this study are from that hole. Refusal occurred at 139.5 mbsf at the boundary between upper Oligocene pelagic sediments and altered basalt. Two additional cores were drilled using the XCB to a total depth of 148 mbsf. The recovery rate for the XCB cores was 71.5%. The contact between altered basalt and Oligocene sediments consists of partly lithified fragments of white foraminifer ooze.

At Sites 871 and 872, the pelagic sediments were soupy and disturbed upon recovery with virtually no preservation of lamination. The sediments consist of very soft and unconsolidated foraminifer and nannofossil-foraminifer ooze that has a clay content between 3% and 8% (Shipboard Scientific Party, 1993a, 1993b). Magnetic susceptibility was generally low or negative, and it was impossible to make a magnetostratigraphic interpretation of the pelagic sediments (Shipboard Scientific Party, 1993a, 1993b).

---

[1] Haggerty, J.A., Premoli Silva, I., Rack, F., and McNutt, M.K. (Eds.), 1995. *Proc. ODP, Sci. Results,* 144: College Station, TX (Ocean Drilling Program).

[2] Geological Institute, University of Copenhagen, Øster Voldgade 10, DK-1350 Copenhagen K, Denmark.

[3] Department of Earth Sciences, University of Cambridge, Downing Street, Cambridge, CB2 3EQ, United Kingdom.

## PRESERVATION OF SEDIMENTS

The pelagic sediments accumulated at Limalok Guyot (Site 871) can be divided into two subunits (Shipboard Scientific Party, 1993a). Subunit IA covers the interval from Section 144-871A-1H-1 to -3H-CC (0–25.1 mbsf). This subunit comprises homogeneous nannofossil foraminifer ooze. Both planktonic foraminifers and nannofossils indicate a Pleistocene to Pliocene biostratigraphic age. Subunit IB from 25.1 to 139.5 mbsf consists of homogeneous foraminifer ooze with winnowed, well-sorted, medium-sized sand texture. The unit is dominated by planktonic foraminifers (95%); nannofossils make up less than 5% of the composition. Biostratigraphic dating of Subunit IB indicates an age from early to middle Miocene. However, micropaleontological studies have demonstrated that sedimentation was episodic and reworking was common. A major hiatus is identified at 21.66 mbsf, between Zone N20 and Subzone N17b. Another hiatus, between Subzone N17a and Zone N12, is evident at 26.72 mbsf, and a minor hiatus at 54.60 mbsf can be identified between Zones N12 and N10. The lower Miocene interval was particularly unsuited for biostratigraphic dating, not only because of upward sediment reworking of zonal marker species, but also because of the lack of well-defined zone fossils (Pearson, this volume). Below 80.5 mbsf (Sections 144-871A-9H-5 to 144-871A-15H-CC), it has not been possible to establish a detailed foraminifer zonation. It has also not been possible to distinguish between Zones N4–N5 and N6–N7 (Fig. 1).

The pelagic sediments at Lo-En Guyot (Site 872) have been divided into two subunits based on the downhole decrease in nannofossil abundance and a corresponding coarsening of the sediment texture (Shipboard Scientific Party, 1993b). The interval analyzed in this study belongs to Subunit IB and consists of an homogeneous foraminifer ooze of fine to medium sand-sized foraminifer tests. Biostratigraphy was especially difficult in Zones N6–N7 (94.25–104.95 mbsf). It has not been possible to differentiate between Zones N6 and N7.

Microfossil preservation is excellent (Plate 1). Estimates made by scanning electron microscopy (SEM) of the amount of secondary calcite on microfossil surfaces were 1%–3% for two samples (Plate 1, Figs. 1 and 8) and less than 1% elsewhere. The internal and external surfaces of microfossils showed no discernable difference in their state of preservation.

## METHODS

### Samples

Downhole caving of the pelagic sediments during coring has introduced a volumetrically significant proportion of contaminants in certain samples (Pearson, this volume), in the worst cases up to 20%. These contaminants were usually of Pleistocene age and thus came from the top of the hole. To avoid analyzing downhole contaminants, we have preferentially used samples of between 20 and 100 individually picked specimens of single foraminifer species presumed to have lived at the time of deposition of the sediment (see Figs. 1–3).

Another kind of sample was prepared to elucidate aspects of the geological reworking history of the sediments. These samples consist of bulk sediment washed and sieved at 150 µm; obvious downhole contaminants were removed manually.

### Analytical Procedures and Precision

For isotopic measurements, the foraminifer tests were fragmented and ultrasonically cleaned in analytically pure acetone for 10 to 15 min. The acetone was then removed by filter paper or pipette. After being dried, the samples were reexamined to ensure that foraminifer tests were the only carbonate material present. For each analysis, 0.4–5.0 mg of calcite was dissolved in 2.5 M HCl. Standard ion exchange techniques were used to separate the strontium. The Sr was dissolved in $HNO_3$ before being mounted on a tantalum filament. Isotope ratios were measured in the dynamic mode on a VG Sector 54 thermal ionization mass spectrometer at the Danish Centre for Isotope Geology at the University of Copenhagen.

Between 50 and 250 ratios were measured for each sample using a beam size of $2 \times 10^{-11}$ Å or $4 \times 10^{-11}$ Å. The average internal standard error for analyses presented in this study is $5 \times 10^{-6}$ (Tables 1 and 2). Samples that ran poorly with an internal standard error of more than $15 \times 10^{-6}$ were prepared and measured again.

Repeated analyses of the NBS-987 standard were performed throughout the study's 6-month period. The average value of the standard was $^{87}Sr/^{86}Sr = 0.710257$, with a standard deviation of 14.8 $\times 10^{-6}$ ($N = 45$).

Duplicate analyses were made on seven samples. These duplicates were cleaned and ion-exchanged independently. The average difference between sample duplicates was $19.8 \times 10^{-6}$. This value gives an estimate of the error associated with the complete processing of samples, including the chemical sample procedure. This value is only slightly greater than the error found on repeated analyses of the NBS-987 standard and is the error quoted for all samples in this study.

## RESULTS

Results of the Sr-isotope analyses are given in Tables 1–2 and Figures 1–3.

From Site 871, 37 samples are plotted vs. depth (Fig. 1), together with the biostratigraphic zonation (foraminifer) and range of the species used for Sr-isotope determinations. The uppermost 20 m of the core shows a linear trend from 0.70906 to 0.70920. A discontinuity in the Sr-isotope record between 20.6 and 25.0 mbsf corresponds to a significant break in deposition between foraminifer Zone N20 and Subzone N17b. The interval from 25 to 80 mbsf shows a weak general trend toward lower $^{87}Sr/^{86}Sr$ values. However, the isotope values exhibit a large spread around this general trend, and several reversals can be seen. Reversals are defined as downward-increasing $^{87}Sr/^{86}Sr$ values. From 80 to 100 mbsf, the trend in Sr-isotope values is well defined and no reversals occur. High variance occurs from 100 mbsf to the bottom of the cap. Only a very weak general trend is visible and several reversals occur. Also, sediment samples generally have lower $^{87}Sr/^{86}Sr$ values than do single-species samples.

Figure 2 shows the Sr-isotope ratios of 16 samples from Site 872 plotted vs. the biostratigraphic zonation and Sr-isotope values. From 90 to 125 mbsf, Sr-isotope values have a decreasing trend. No overall trend in the data are evident from 120 mbsf to the bottom of the pelagic cap, and several reversals were recognized. One reversal between 135 and 145 mbsf is especially evident.

## DISCUSSION

### Isotope Ages

Strontium isotope ages were determined using four different Sr-isotope/age regressions following the methods of Hodell et al. (1991) and Oslick et al. (1994). All calculated ages are shown in Tables 1 and 2 and in Figure 3. For Sr-isotope/age assignments, only specimens of single foraminifer species were used. The ages obtained were calculated under the assumption that these $^{87}Sr/^{86}Sr$ measurements were, to a lesser extent than the sediment samples, affected by sediment reworking or downhole contaminants. In other words, they represent the best estimate of sediment age.

The regression equation of Hodell et al. (1991) was used for the Pleistocene–Pliocene part of the Hole 871A Sr-isotope curve: age = 11,931.82 – ($^{87}Sr/^{86}Sr$)16,824.84. This equation can also be written as age = –0.132 $\delta^{87}Sr$, where $\delta^{87}Sr$ is the $^{87}Sr/^{86}Sr$ of the sample in per mil deviation from modern seawater. The equation covers the time interval from 0 to 2.5 Ma and is based on Sr-isotope values and a magnetostratigraphic chronology from DSDP Site 588. The Geomagnetic Polarity Time Scale (GPTS) used at this site is from Berggren et al. (1985). We use the delta notation form because it is independent of interlaboratory differences in measured NBS-987 values. By using this approach, we

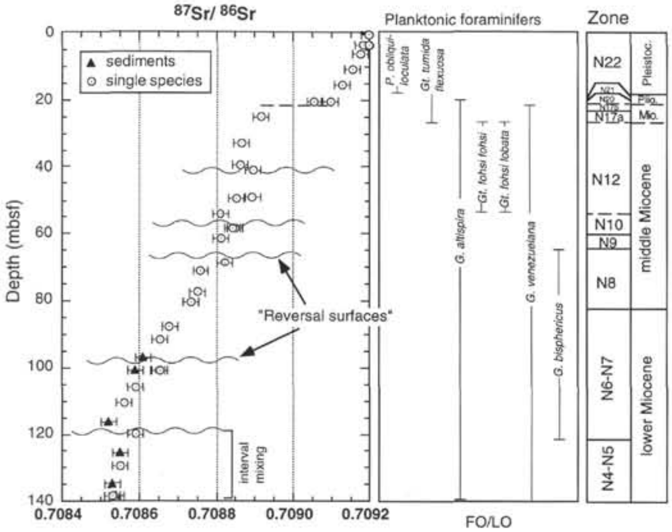


Figure 1. Measured $^{87}Sr/^{86}Sr$ vs. depth for sediments (picked clean of downhole contaminants) and single-species foraminifer samples in Hole 871A. Only $^{87}Sr/^{86}Sr$ values with internal precision better than 20 ppm are shown (Table 1). Foraminifer zones and species used for Sr-isotope measurements are shown to the right.

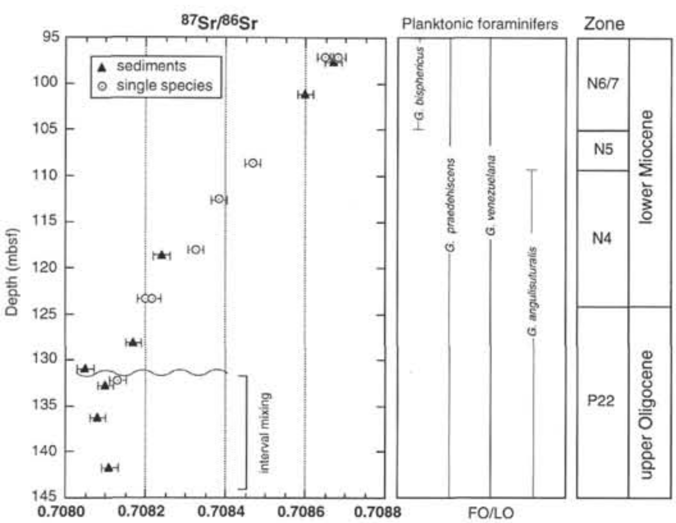


Figure 2. Measured $^{87}Sr/^{86}Sr$ vs. depth for sediments (picked clean of downhole contaminants) and single-species foraminifer samples in Hole 872C. Only $^{87}Sr/^{86}Sr$ values with internal precision better than 20 ppm are shown (Table 2). Foraminifer zones and species used for Sr-isotope measurements are shown to the right.

were sure to get a zero age for the sample with the highest $^{87}Sr/^{86}Sr$ value. As a reference for modern seawater, we used our highest measured Sr-isotope value from Section 144-871A-1H-3 (0.70920). Hodell et al. (1991) use a modern seawater value of 0.709172; thus, our value is 0.000028 higher.

For the middle Miocene, we used the regression of Oslick et al. (1994): age = 31,799.78 – ($^{87}Sr/^{86}Sr$)44,843.005. This equation is valid from 15.2 to 9.2 Ma and corresponds to $^{87}Sr/^{86}Sr$ values of 0.708930 to 0.708789. The equation is based on data from ODP Hole 747A, and Sr-isotope ages are calibrated to the GPTS of Berggren et al. (1985). This makes the equation directly comparable to the Pleistocene regression mentioned above and to the planktonic biostratigraphy used in this study. Oslick et al. (1994) measured NBS-987

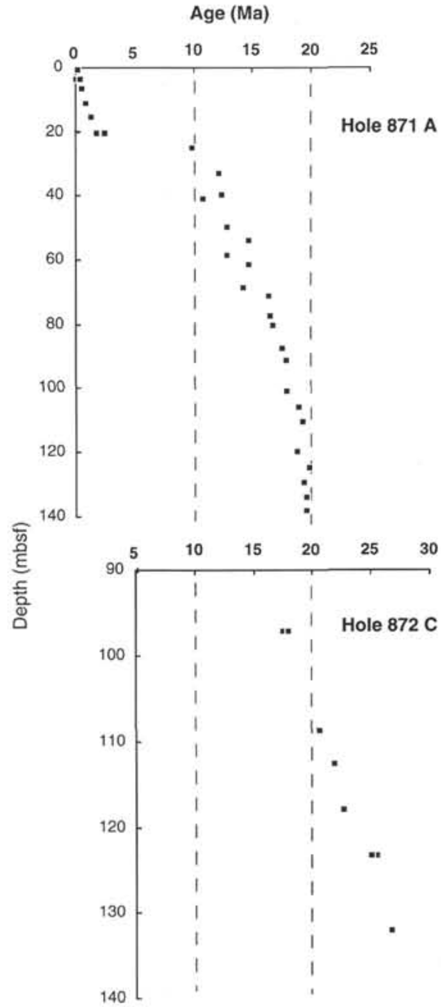


Figure 3. Age vs. depth for single-species planktonic foraminifers. Ages are calculated using the Sr-isotope/age regressions published by Hodell et al. (1991) and Oslick et al. (1994).

$^{87}Sr/^{86}Sr$ as 0.710255, and we reduced our data by 0.000002 to make the values compatible. Obviously, when using the NBS-987 correction instead of modern seawater, we introduced an error when comparing with the Pleistocene segment of the curve. This error, however, is small compared with the gap of more than 5 Ma between the two line segments (Fig. 3).

In the time interval from 15.6 to 22.8 Ma (lower to lowermost middle Miocene), corresponding to $^{87}Sr/^{86}Sr$ values from 0.7087889 to 0.708305, the following Sr-isotope/age regression was used: age = 10,258.53 – ($^{87}Sr/^{86}Sr$)14,450.87 (Oslick et al., 1994).

The final Sr-isotope/age regression used covered the upper Oligocene interval (23.2–28.0 Ma) or $^{87}Sr/^{86}Sr$ values from 0.708304 to 0.708065: age = 13,803.52 – ($^{87}Sr/^{86}Sr$)19,455.25. This equation has been constructed using the more recent GPTS developed by Cande and Kent (1992). The difference between the GPTS of Berggren et al. (1985) is negligible in this time interval and can be disregarded (Oslick et al., 1994).

The age calculations, plotted vs. depth, for the pelagic caps at Sites 871 and 872 are shown in Figure 3. The highest age found in Hole 871A is 19.8 Ma, which is, therefore, the Sr-isotope minimum age of initial pelagic sedimentation on Limalok Guyot. There is an overall trend from 19.8 to 9.9 Ma, with an apparent mixing in the interval from 140 to 120 mbsf. This is followed by a major hiatus from 9.9 to 2.4 Ma. However, the curve contains several age reversals, which indicate that

**Table 1. Samples, depths, planktonic foraminifer zonation, Sr-isotope values, and calculated Sr-isotope age from Hole 871A.**

| Core, section, interval (cm) | Species | Zone | Depth (mbsf) | $^{87}Sr/^{86}Sr$ | ±2 SE | Calculated Sr-isotope ages (Ma) |
|---|---|---|---|---|---|---|
| 144-871A- | | | | | | |
| 1H-1, 59–61 | *Pulleniatina obliquiloculata* | N22 | 0.6 | 0.7091961 | 0.000009 | 0.1 |
| 1H-3, 59–61 | *Pulleniatina obliquiloculata* | N22 | 3.5 | 0.7092000 | 0.000013 | 0.0 |
| 1H-3, 59–61 | *Pulleniatina obliquiloculata* | N22 | 3.5 | 0.7091816 | 0.000010 | 0.3 |
| 1H-5, 59–61 | *Pulleniatina obliquiloculata* | N22 | 6.5 | 0.7091757 | 0.000006 | 0.4 |
| 2H-3, 59–61 | *Pulleniatina obliquiloculata* | N22 | 11.1 | 0.7091551 | 0.000007 | 0.8 |
| 2H-6, 59–61 | *Pulleniatina obliquiloculata* | N22 | 15.6 | 0.7091276 | 0.000006 | 1.2 |
| 3H-3, 60–62 | *Globorotalia tumida flexuosa* | N19/20 | 20.6 | 0.7090973 | 0.000006 | 1.7 |
| 3H-3, 60–62 | *Globorotalia tumida flexuosa* | N19/20 | 20.6 | 0.7090559 | 0.000013 | 2.4 |
| 3H-6, 60–62 | *Dentoglobigerina altispira* | N17b | 25.1 | 0.7089170 | 0.000009 | 9.9 |
| 4H-4, 59–61 | *Globorotalia fohsi lobata* | N12 | 31.6 | 0.7088312 | 0.000038 | |
| 4H-5, 59–61 | *Globorotalia fohsi lobata* | N12 | 33.1 | 0.7088675 | 0.000007 | 12.1 |
| 5H-3, 59–61 | *Globorotalia fohsi lobata* | N12 | 39.6 | 0.7088621 | 0.000011 | 12.3 |
| 5H-4, 59–61 | *Globorotalia fohsi fohsi* | N12 | 41.1 | 0.7088969 | 0.000006 | 10.8 |
| 6H-3, 60–62 | *Globorotalia fohsi fohsi* | N12 | 49.1 | 0.7088950 | 0.000026 | |
| 6H-3, 124–126 | *Globorotalia fohsi fohsi* | N12 | 49.8 | 0.7088210 | 0.000034 | |
| 6H-3, 124–126 | *Globorotalia fohsi fohsi* | N12 | 49.8 | 0.7088522 | 0.000011 | 12.8 |
| 6H-6, 124–126 | *Dentoglobigerina altispira* | N12 | 54.3 | 0.7088115 | 0.000011 | 14.6 |
| 7H-3, 59–61 | *Dentoglobigerina altispira* | N10 | 58.6 | 0.7088508 | 0.000027 | |
| 7H-3, 59–61 | *Dentoglobigerina altispira* | N10 | 58.6 | 0.7088439 | 0.000011 | 13.1 |
| 7H-5, 59–61 | *Dentoglobigerina altispira* | N9 | 61.6 | 0.7088288 | 0.000037 | |
| 7H-5, 59–61 | *Dentoglobigerina altispira* | N9 | 61.6 | 0.7088120 | 0.000010 | 14.6 |
| 8H-3, 125–127 | *Dentoglobigerina altispira* | N8 | 68.8 | 0.7087485 | 0.000033 | |
| 8H-3, 125–127 | *Dentoglobigerina altispira* | N8 | 68.8 | 0.7088223 | 0.000009 | 14.1 |
| 8H-5, 59–61 | *Globigerinoides bispericus* | N8 | 71.1 | 0.7087601 | 0.000013 | 16.3 |
| 9H-3, 59–61 | *Dentoglobigerina altispira* | N8 | 77.6 | 0.7087525 | 0.000007 | 16.4 |
| 9H-5, 59–61 | *Dentoglobigerina altispira* | N8 | 80.6 | 0.7087355 | 0.000014 | 16.7 |
| 10H-3, 124–126 | *Globoquadrina venezuelana* | N6–N7 | 87.8 | 0.7086802 | 0.000016 | 17.5 |
| 10H-6, 59–61 | *Dentoglobigerina altispira* | N6–N7 | 91.6 | 0.7086541 | 0.000007 | 17.9 |
| 11H-3, 124–126 | Sediment clean of contaminants | N6–N7 | 97.3 | 0.7086138 | 0.000009 | |
| 11H-6, 59–61 | *Dentoglobigerina altispira* | N6–N7 | 101.1 | 0.7086500 | 0.000018 | 17.9 |
| 11H-6, 59–61 | *Dentoglobigerina altispira* | N6–N7 | 101.1 | 0.7086539 | 0.000014 | 17.9 |
| 11H-6, 60–62 | Sediment clean of contaminants | N6–N7 | 101.1 | 0.7085903 | 0.000018 | |
| 12H–3, 59–61 | *Dentoglobigerina altispira* | N6–N7 | 106.1 | 0.7085870 | 0.000011 | 18.8 |
| 12H-6, 59–61 | *Dentoglobigerina altispira* | N6–N7 | 110.6 | 0.7085607 | 0.000013 | 19.2 |
| 13H-3, 58-60 | *Dentoglobigerina altispira* | N6–N7 | 115.6 | 0.7085748 | 0.000047 | |
| 13H-3, 124–126 | Sediment clean of contaminants | N6–N7 | 116.3 | 0.7085193 | 0.000010 | |
| 13H-6, 58–60 | *Dentoglobigerina altispira* | N6–N7 | 120.1 | 0.7085942 | 0.000011 | 18.7 |
| 14H-3, 60–62 | *Dentoglobigerina altispira* | N4–N5 | 125.1 | 0.7085221 | 0.000030 | 19.8 |
| 14H-3, 125–127 | Sediment clean of contaminants | N4–N5 | 125.8 | 0.7085550 | 0.000009 | |
| 14H-6, 60–61 | *Dentoglobigerina altispira* | N4–N5 | 129.6 | 0.7085524 | 0.000010 | 19.3 |
| 15H–3, 59–61 | *Dentoglobigerina altispira* | N4–N5 | 134.1 | 0.7085390 | 0.000030 | 19.5 |
| 15H-3, 124–126 | Sediment clean of contaminants | N4–N5 | 134.8 | 0.7085341 | 0.000011 | |
| 15H-6, 59–61 | *Dentoglobigerina altispira* | N4–N5 | 138.6 | 0.7085345 | 0.000017 | 19.6 |
| 15H-6, 59–61 | Sediment clean of contaminants | N6–N7 | 138.6 | 0.7085420 | 0.000013 | |

Notes: For single-species samples, names of foraminifer species used for analysis are given. See range of foraminifer species in Figure 1. SE = standard error.

**Table 2. Samples, depths, planktonic foraminifer zonation, Sr-isotope values, and calculated Sr-isotope ages from Hole 872C.**

| Core, section, interval (cm) | Species | Zone | Depth (mbsf) | $^{87}Sr/^{86}Sr$ | ±2 SE | Calculated Sr-isotope ages (Ma) |
|---|---|---|---|---|---|---|
| 144-872C- | | | | | | |
| 11H-3, 20–22 | *Globigerinoides bisphericus* | N6–N7 | 97.2 | 0.7086829 | 0.000027 | 17.4 |
| 11H-3, 20–22 | *Globigerinoides bisphericus* | N6–N7 | 97.2 | 0.7086480 | 0.000016 | 17.9 |
| 11H-3, 70–72 | Sediment clean of contaminants | N6–N7 | 97.7 | 0.7086717 | 0.000013 | |
| 11H-6, 20–21 | Sediment clean of contaminants | N6–N7 | 101.2 | 0.7085983 | 0.000017 | |
| 13H-3, 20–22 | *Gloquadrina praedehiscens* | N5 | 108.7 | 0.7084673 | 0.000034 | 20.6 |
| 13H-3, 20–22 | *Gloquadrina praedehiscens* | N5 | 108.7 | 0.7084674 | 0.000009 | 20.6 |
| 13H-6, 20–22 | *Gloquadrina praedehiscens* | N4 | 112.7 | 0.7083838 | 0.000010 | 21.8 |
| 14H-3, 20–22 | *Gloquadrina praedehiscens* | N4 | 118.1 | 0.7083251 | 0.000010 | 22.6 |
| 14H-3, 78–80 | Sediment clean of contaminants | N4 | 118.7 | 0.7082395 | 0.000013 | |
| 14H-7, 20–22 | *Gloquadrina venezuelana* | N4 | 123.4 | 0.7081958 | 0.000008 | 25.4 |
| 14H-7, 20–22 | *Gloquadrina venezuelana* | N4 | 123.4 | 0.7082174 | 0.000008 | 25.0 |
| 15H-3, 78–80 | Sediment clean of contaminants | P22 | 128.1 | 0.7081672 | 0.000014 | |
| 15H-6, 20–22 | Sediment clean of contaminants | P22 | 131.0 | 0.7080466 | 0.000010 | |
| 16H-3, 20–22 | *Globigerina angulisuturalis* | P22 | 132.2 | 0.7081321 | 0.000011 | 26.7 |
| 16H-3, 78–90 | Sediment clean of contaminants | P22 | 132.8 | 0.7080971 | 0.000008 | |
| 16H-6, 78–80 | *Globigerina angulisuturalis* | P22 | 136.3 | 0.7081098 | 0.000042 | |
| 16H-6, 78–80 | Sediment clean of contaminants | P22 | 136.3 | 0.7080755 | 0.000010 | |
| 17X-2, 20–22 | *Globigerina angulisuturalis* | P22 | 141.2 | 0.7080503 | 0.000059 | |
| 17X-2, 78–80 | Sediment clean of contaminants | P22 | 141.8 | 0.7081144 | 0.000008 | |

Notes: For single-species samples, names of foraminifer species are given. See range of foraminifer species in Figure 2. SE = standard error.

reworking of sediments has occurred in certain intervals (see discussion below). In Hole 872C, the highest age obtained is 26.7 Ma. This must also be regarded as a minimum date for initial pelagic sedimentation on Lo-En Guyot. No age reversals were found at Hole 872C. The plot of Sr-isotope ages vs. depth yields a straight line, indicating a relatively constant sedimentation rate from 26.7 to 17.4 Ma. Altogether, the Sr isotopes represent a rough chronology for the two sites. There are general trends for both sites. However, Sr ages must be used with caution, especially in intervals that have many age reversals.

### Reworking History

It has been possible to distinguish two kinds of reworking. The first involves obvious erosion and development of discontinuity surfaces. It can be recognized by gaps in the Sr-isotope curve. The second involves reworking where older sediments are deposited above younger. This kind of reworking can be recognized as reversals in the Sr-isotope vs. depth and age vs. depth plots. Also, an inconsistency between a bulk sediment sample and a single-species sample from the same level suggests a certain proportion of older reworked sediment components with lower $^{87}Sr/^{86}Sr$ values at this level.

The pelagic cap at Limalok Guyot (Site 871) is the best studied of the two sites. The lower Miocene, corresponding to the lowermost 20 m of the cap, was particularly unsuited for biostratigraphic interpretation (Fig. 1), not only because of upward sediment reworking of zonal marker species, but also because of the lack of well-defined zonal fossils (Pearson, this volume). It has not been possible, therefore, to make a biostratigraphic distinction between planktonic foraminifer Zones N4 and N5 (Fig. 1). There is no significant trend from lower to higher Sr-isotope values and no significant difference between bulk sediment samples and single-species foraminifer samples. Therefore, we concluded that the intervals consist of thoroughly mixed sediments. As mentioned previously, Sr-isotope ages obtained from this mixed interval must be considered as minimum ages. From 120 mbsf to the discontinuity surface at 20.6 mbsf, the frequency of reversals increases upward (Figs. 1 and 3). Altogether, five "reversal surfaces" have been observed, indicating reworking and deposition of older sediments on top of younger sediments. From 60 to 20.6 mbsf, Sr-isotope values show a large scatter around a generally upward-increasing trend. Two hiatuses in the same interval are evident from the biostratigraphy: one at 54.6 mbsf where Zone N11 is missing and one at 26.7 mbsf where Zones N13–N16 are missing. These suggest a high-energy depositional environment probably caused by ocean current activity. The discontinuity surface at 20.6 mbsf indicates a major period of erosion. No sediments from 9.9 to 2.4 Ma, corresponding to Zones N18 and N19, were preserved (Figs. 2–3). In the uppermost 20 m (0–20.6 mbsf) of the pelagic cap, Sr-isotope values have a well-defined trend. The measured $^{87}Sr/^{86}Sr$ values from 0.70905 to 0.70920 correspond to the seawater Sr values for the Pleistocene (Zone N22; Hodell et al., 1991) and indicate negligible reworking or mixing in this interval.

Only the initial 50 m of pelagic sediments has been studied at Lo-En Guyot (Site 872). As for Limalok, the lowermost 20 m shows several reversals and an inconsistency between single-species foraminifer samples and sediment samples (Fig. 2). This suggests severe reworking and mixing of sediments. The rest of the studied part of the core has a well-defined trend, and no significant inconsistency between single-species and sediment samples occur. The Sr-isotope/age assignments have been more successful for Lo-En than for Limalok guyot. This suggests that single-species foraminifer samples give a reliable estimate of the sediment age for Lo-en Guyot (Fig. 3).

## CONCLUSIONS

The establishment of a detailed chronostratigraphy for the Leg 144 pelagic caps was problematic because major reworking in certain intervals caused difficulties for biostratigraphic age assignment. Furthermore, magnetostratigraphy was unavailable because of the nature of the sediments.

The pelagic caps studied contain well-preserved foraminifer faunas (Pearson, this volume). However, reworking was so severe in these sediments that it was not possible to construct a detailed Sr-isotope seawater curve. Therefore, we used Sr isotopes not only as an additional stratigraphic tool but mainly to provide an estimate of the extent and timing of sediment reworking in these sections. The Sr-isotope data have shown that great caution should be taken in the interpretation of all geochemical parameters measured in pelagic caps from the western Pacific guyots.

For both pelagic caps, reworking seems to be most significant in the oldest part of the sediment cover directly above the carbonate platform, suggesting that reworking is an original feature associated with sediment deposition and not an artifact caused by the drilling process. At Limalok Guyot (Site 871), the minimum age of pelagic sedimentation was calculated to be 19.8 Ma, whereas pelagic sedimentation initiated at 26.7 Ma at Lo-En Guyot (Site 872). At Limalok Guyot (Site 871), an interval from 14.2 to 2.4 Ma that had frequent reworking was also recognized.

The material in this study is too sparse to suggest a reliable cause of sediment reworking, but some explanations could be proposed: (1) wave activity affected the guyots as they subsided below wave base, and (2) ocean currents at greater depths affected the guyots after subsidence below wave base.

## ACKNOWLEDGMENTS

We thank Paul M. Holm and Svend Pedersen from the Danish Centre of Isotope Geology for help with the Sr-isotope analyses. The mass spectrometer facilities were supported by Danish Research Grant No. 6.20.62.10.1. For critical reviews of the manuscript, we wish to thank David A. Hodell and J.M. McArthur.

### REFERENCES*

Berggren, W.A., Kent, D.V., Flynn, J.J., and Van Couvering, J., 1985. Neogene geochronology and chronostratigraphy. *In* Snelling, N.J. (Ed.), *The Chronology of the Geological Record.* Geol. Soc. London Mem., 10:211–250.

Burke, W.H., Denison, R.E., Hetherington, E.A., Koepnick, R.B., Nelson, H.F., and Otto, J.B., 1982. Variation of seawater $^{87}Sr/^{86}Sr$ throughout Phanerozoic time. *Geology,* 10:516–519.

Cande, S.C., and Kent, D.V., 1992. A new geomagnetic polarity time scale for the Late Cretaceous and Cenozoic. *J. Geophys. Res.,* 97:13917–13951.

DePaolo, D.J., 1986. Detailed record of the Neogene Sr isotopic evolution of seawater from DSDP Site 590B. *Geology,* 14:103–106.

Hess, J., Stott, L.D., Bender, M.L., Kennett, J.P., and Schilling, J.-G., 1989. The Oligocene marine microfossil record: age assessments using strontium isotopes. *Paleoceanography,* 4:655–679.

Hodell, D.A., Mead, G.A., and Mueller, P.A., 1990. Variation in the strontium isotopic composition of seawater (8 Ma to present): implications for chemical weathering rates and dissolved fluxes to the oceans. *Chem. Geol. (Isotope Geosci. Sect.),* 80:291–307.

Hodell, D.A., Mueller, P.A., and Garrido, J.R., 1991. Variations in the strontium isotopic composition of seawater during the Neogene. *Geology,* 19:24–27.

Hodell, D.A., Mueller, P.A., McKenzie, J.A., and Mead, G.A., 1989. Strontium isotope stratigraphy and geochemistry of the late Neogene ocean. *Earth Planet. Sci. Lett.,* 92:165–178.

Hodell, D.A., and Woodruff, F., 1994. Variations in the strontium isotopic ratio of seawater during the Miocene: sratigraphic and geochemical implications. *Paleoceanography,* 9:405–426.

Kennett, J.P., and Srinivasan, M.S., 1983. *Neogene Planktonic Foraminifera: A Phylogenetic Atlas:* Stroudsburg, PA (Hutchinson Ross).

Koepnick, R.B., Burke, W.H., Denison, R.E., Hetherington, E.A., Nelson, H.F., Otto, J.B., and Waite, L.E., 1985. Construction of the seawater

* Abbreviations for names of organizations and publications in ODP reference lists follow the style given in *Chemical Abstracts Service Source Index* (published by American Chemical Society).

$^{87}Sr/^{86}Sr$ curve for the Cenozoic and Cretaceous: supporting data. *Chem. Geol. (Isotope Geosci. Sect.),* 58:55–81.

Koepnick, R.B., Denison, R.E., and Dahl, D.A., 1988. The Cenozoic seawater $^{87}Sr/^{86}Sr$ curve: data review and implications for correlations of marine strata. *Paleoceanography,* 3:743–756.

Miller, K.G., Feigenson, M.D., Kent, D.V., and Olsson, R.K., 1988. Upper Eocene to Oligocene isotope ($^{87}Sr/^{86}Sr$, $\delta^{18}O$, $\delta^{13}C$) standard section, Deep Sea Drilling Project Site 522. *Paleoceanography,* 3:223–233.

Miller, K.G., Feigenson, M.D., Wright, J.D., and Clement, B.M., 1991. Miocene isotope reference section, Deep Sea Drilling Project Site 608: an evaluation of isotope and biostratigraphic resolution. *Paleoceanography,* 6:33–52.

Oslick, J.S., Miller, K.G., and Feigenson, M.D., 1994. Oligocene-Miocene strontium isotopes: stratigraphic revision and correlation to an inferred glacioeustatic record. *Paleoceanography,* 9:427–443.

Shipboard Scientific Party, 1993a. Site 871. *In* Premoli Silva, I., Haggerty, J., Rack, F., et al., *Proc. ODP, Init. Repts.,* 144: College Station, TX (Ocean Drilling Program), 41–103.

———, 1993b. Site 872. *In* Premoli Silva, I., Haggerty, J., Rack, F., et al., *Proc. ODP, Init. Repts.,* 144: College Station, TX (Ocean Drilling Program), 105–144.

**Date of initial receipt: 4 February 1994**
**Date of acceptance: 15 September 1994**
**Ms 144SR-051**

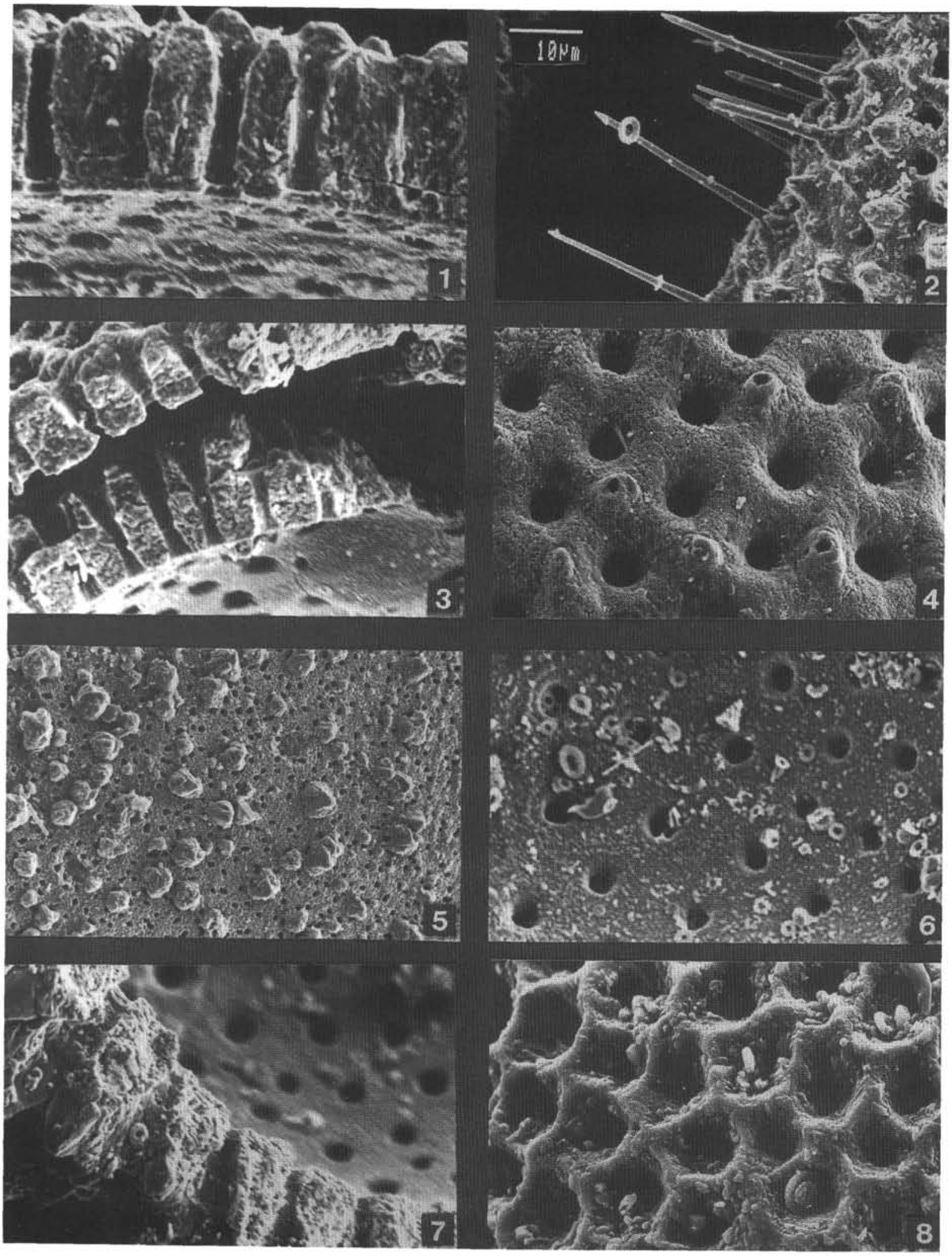


Plate 1. Preservation of planktonic foraminifers from Sites 871 and 872. **1.** Sample 144-871A-1H-4, 59–61 cm, Pleistocene (Zone N22). Deliberately broken test. Original granular calcite texture preserved. **2.** Sample 144-871A-7H-3, 59–61 cm, middle Miocene (Zone N9). Preservation of delicate spines in *Globigerinella praesiphonifera.* **3.** Sample 144-871A-7H-5, 59–61 cm, middle Miocene (Zone N9). Deliberately broken test. Good preservation. **4.** Sample 144-871A-7H-CC, 59–61 cm, middle Miocene (Zone N9). Surface ultrastructure of *Globigerinoides trilobus* shows excellent preservation of wall texture, including pores and spine bases. **5.** Sample 144-871A-12H-CC, lower Miocene (Zones ?N4/N5). Surface ultrastructure of *Globigerinella* sp. Small pustules and pores are part of original wall texture. **6.** Sample 144-871A-14H-2, 59–61 cm, lower Miocene (Zones ?N4/N5). Surface ultrastructure of *Globigerina glutinata.* Small pustules are part of original wall texture. **7.** Sample 144-871A-15H-6, 59–61 cm, lower Miocene (Zones ?N4/N5). Deliberately broken test. No internal calcite precipitate exists, but the internal texture shows minor signs of diagenetic recrystallization. **8.** Sample 144-872B-15H-5, 59–61 cm, late Oligocene (Zone P22). Surface ultrastructure of cancellate *Catapsydrax dissimilis.* Preservation is generally good, but minor signs of recrystallization can be observed.